AGU PUBLICATIONS

Geophysical Research Letters

RESEARCH LETTER
10.1002/2016GL071645

Key Points:
- Iceberg meltwater flux is computed using an iceberg model forced with conditions from (i) GCM output and (ii) an observational state estimate
- Large-scale differences in meltwater fluxes are driven by relatively small scale differences in ocean currents
- The impact of a high wind bias in the GCM is reduced through compensating effects of wind-driven erosion and drift

Supporting Information:
- Supporting Information S1

Correspondence to:
T. J. W. Wagner,
tjwagner@ucsd.edu

Citation:
Wagner, T. J. W., and I. Eisenman (2017), How climate model biases skew the distribution of iceberg meltwater, *Geophys. Res. Lett.*, *44*, doi:10.1002/2016GL071645.

Received 21 OCT 2016
Accepted 17 FEB 2017
Accepted article online 3 MAR 2017

How climate model biases skew the distribution of iceberg meltwater

Till J. W. Wagner[1] **and Ian Eisenman**[1]

[1] Scripps Institution of Oceanography, University of California San Diego, La Jolla, California, USA

Abstract The discharge of icebergs into the polar oceans is expected to increase over the coming century, which raises the importance of accurate representations of icebergs in global climate models (GCMs) used for future projections. Here we analyze the prospects for interactive icebergs in GCMs by forcing an iceberg drift and decay model with circulation and temperature fields from (i) state-of-the-art GCM output and (ii) an observational state estimate. The spread of meltwater is found to be smaller for the GCM than for the observational state estimate, despite a substantial high wind bias in the GCM—a bias that is similar to most current GCMs. We argue that this large-scale reduction in the spread of meltwater occurs primarily due to localized differences in ocean currents, which may be related to the coarseness of the horizontal resolution in the GCM. The high wind bias in the GCM is shown to have relatively little impact on the meltwater distribution, despite Arctic iceberg drift typically being dominated by the wind forcing. We find that this is due to compensating effects between faster drift under stronger winds and larger wind-driven wave erosion. These results may have implications for future changes in the Atlantic meridional overturning circulation simulated with iceberg-enabled GCMs.

Plain Language Summary Recent reductions in the volume of the polar ice sheets highlight the importance of the question how ice sheet meltwater impacts the large-scale ocean circulation and global climate. For example, it has been argued that increased meltwater from Greenland will slow down the Atlantic meridional overturning circulation (AMOC) in the coming decades. The likelihood of this scenario depends on where the meltwater is released at the ocean surface. Icebergs, which carry up to half of this meltwater, play a crucial role in transporting meltwater equatorward in the North Atlantic. Our results suggest that climate models that include icebergs will underestimate this equatorward transport of meltwater, with potentially far-reaching implications for the AMOC.

1. Introduction

A large fraction of the freshwater flux from the polar ice sheets into the global oceans occurs in the form of iceberg calving. Icebergs have been estimated to contribute more than 510 Gt/yr of freshwater from the Greenland ice sheet in recent years [*Enderlin et al.*, 2014] and more than 1300 Gt/yr from Antarctica [*Depoorter et al.*, 2013]. Iceberg calving rates are expected to further increase with rising ice sheet mass loss during the coming century [*Rignot et al.*, 2011; *Joughin et al.*, 2014; *Liu et al.*, 2015]. This may have far-reaching implications for the global climate system, since icebergs not only affect local water columns [*Stern et al.*, 2015] and ecosystems [*Vernet et al.*, 2012; *Smith et al.*, 2013; *Duprat et al.*, 2016] but their meltwater flux can also impact the large-scale ocean circulation [*Sierro et al.*, 2005; *Martin and Adcroft*, 2010; *Jongma et al.*, 2013; *van den Berk and Drijfhout*, 2014]. Feedbacks associated with these effects may in turn influence the stability of the ice sheets [e.g., *Bügelmayer et al.*, 2015].

Explicitly representing interactive icebergs in global climate models (GCMs) is a significant challenge facing the climate modeling community. With efforts to address this currently underway [e.g., *Jongma et al.*, 2009; *Martin and Adcroft*, 2010; *Hunke and Comeau*, 2011; *Marsh et al.*, 2015; *Merino et al.*, 2016; *Stern et al.*, 2016], it is important to determine the sensitivities of the dynamics and thermodynamics governing iceberg drift and decay and their interplay with the climate system. Otherwise, GCM biases that affect the distribution of iceberg meltwater may introduce unknown errors in large-scale ocean circulation and climate projections. In this study, we investigate the effects that such GCM biases may have on iceberg meltwater fluxes.

2. Iceberg Drift and Decay Simulations

In order to analyze the prospects for fully interactive icebergs in GCMs, here we consider a simpler scenario in which icebergs are forced by specified wind, ocean current, and sea surface temperature (SST) fields. We compare results that use fields from a GCM simulation with results that use fields from an observational state estimate. We further consider the impact of switching between different widely used melt representations.

2.1. Observational State Estimate and GCM Input Fields

For the GCM fields, we use a twentieth century simulation that was carried out with the National Center for Atmospheric Research Community Climate System Model version 4 (CCSM4) [*Gent et al.*, 2011] as one of the "Historical" experiments for the Coupled Model Intercomparison Project Phase 5 (CMIP5) [*Taylor et al.*, 2012]. This CCSM4 simulation has a horizontal resolution of approximately 1° in the atmosphere and nominally 1° in the ocean.

We compare this with the global ocean state estimate from the Estimating the Circulation and Climate of the Ocean Phase II (ECCO2) project [*Menemenlis et al.*, 2008]. The ECCO2 state estimate is calculated using a least squares fit of available observational data to an ocean general circulation model with a mean horizontal resolution of 18 km. The ocean is forced with surface winds from the Japanese 25 year Reanalysis (JRA-25) [*Onogi et al.*, 2007], which has approximately 1° native resolution and is interpolated onto the ECCO2 grid. For both the CCSM4 and ECCO2 results, we consider SSTs, surface currents, and surface winds over the 14 year period from 1 January 1992 (the beginning of the ECCO2 dataset) to 31 December 2005 (the end of the CCSM4 Historical simulation). We look at long-term mean conditions by averaging iceberg freshwater release over the 14 year period. CCSM4 simulates internal variability of the coupled climate system that is unconstrained by observations, but the 1992–2005 time period is sufficiently long to remove much of this variability in the fields of interest, as indicated in Figure S1 in the supporting information.

2.2. Iceberg Model

In order to obtain iceberg trajectories under specified ocean currents and winds, we use a recently developed Lagrangian iceberg drift model, which evolves the velocity of an iceberg, $\vec{v}_i$, under the influence of air drag, water drag, the pressure gradient force, and the Coriolis force [*Wagner et al.*, 2016]. This formulation is somewhat idealized compared to previous iceberg models [e.g., *Bigg et al.*, 1997; *Gladstone et al.*, 2001; *Roberts et al.*, 2014], which allows an analytical solution for iceberg velocity as a function of surface air velocity, $\vec{v}_a$, and surface water velocity, $\vec{v}_w$. The solution can be written as

$$\vec{v}_i = \vec{v}_w + \gamma\left(-\alpha\hat{k}\times\vec{v}_a + \beta\vec{v}_a\right), \tag{1}$$

where γ is a dimensionless parameter that describes the relative importance of water drag versus air drag,

$$\gamma \equiv \left[\frac{\rho_a(\rho_w-\rho_i)}{\rho_w\rho_i}\frac{C_a}{C_w}\right]^{1/2}, \tag{2}$$

with ρ_a, ρ_w, ρ_i, C_a, and C_w being the densities of air, water, and ice, and the drag coefficients of air and water, respectively. The dimensionless parameters α and β can be written as

$$\begin{aligned}\alpha &\equiv \frac{1}{2\Lambda^3}\left(\sqrt{1+4\Lambda^4}-1\right),\\ \beta &\equiv \frac{1}{\sqrt{2}\Lambda^3}\left[\left(1+\Lambda^4\right)\sqrt{1+4\Lambda^4}-3\Lambda^4-1\right]^{1/2},\end{aligned} \tag{3}$$

where $\Lambda \equiv \gamma\, C_w|\vec{v}_a| / \left(\pi f S\right)$, with f being the Coriolis parameter and $S \equiv L\,W/(L+W)$ being the harmonic mean horizontal length of the iceberg. Icebergs are considered to be cuboids of length L, width W, and height H. Since $\vec{v}_i$ depends on iceberg size through α and β, the drift model is coupled to a representation of iceberg decay (see below), and the trajectories will be computed for a range of different initial size classes.

The solution (1)–(3) enables us to efficiently compute large numbers of iceberg trajectories from specified circulation fields, and it allows insight into the physical processes that drive iceberg drift. The derivation of equations (1)–(3) is given in *Wagner et al.* [2016], along with the parameter values and simplifying assumptions which include neglecting irregular iceberg shapes and variations in the vertical ocean velocity profile.

This model [*Wagner et al.*, 2016] accounts for iceberg decay using a representation adapted from *Bigg et al.* [1997], which includes three ablation processes. These are (i) wind-driven wave erosion, M_e; (ii) turbulent

basal melt, M_b; and (iii) sidewall erosion from buoyant convection, M_v. The iceberg dimensions are evolved separately in the model according to $dL/dt = dW/dt = M_e + M_v$ and $dH/dt = M_b$, with iceberg volume given by $V = L\,W\,H$. The ablation processes are represented as

$$\begin{aligned} M_e &= a_1 |\vec{v}_a|^{1/2} + a_2 |\vec{v}_a|, \\ M_v &= b_1\, T_w + b_2\, T_w^2, \\ M_b &= c\, |\vec{v}_w - \vec{v}_i|^{0.8}\, (T_w - T_i)\, L^{-0.2}, \end{aligned} \tag{4}$$

where $a_1 = 8.7 \times 10^{-6}$ m$^{1/2}$ s$^{-1/2}$ and $a_2 = 5.8 \times 10^{-7}$ are related to the sea state, $b_1 = 8.8 \times 10^{-8}$ m s^{-1} °C^{-1}, $b_2 = 1.5 \times 10^{-8}$ m s^{-1} °C^{-2}, $c = 6.7 \times 10^{-6}$ m$^{-2/5}$ s$^{-1/5}$ °C^{-1}, T_i is the temperature of the ice which is taken to be fixed at −4°C, and T_w is the SST. The main difference compared with the model of *Bigg et al.* [1997] is that we use an updated iceberg rollover criterion [*Wagner et al.*, 2017], since the widely used rollover criterion of *Weeks and Mellor* [1978] has recently been found to contain errors [*Wagner et al.*, 2017].

In agreement with previous modeling studies [see, e.g., *Gladstone et al.*, 2001], it will be shown below that the dominant ablation term is the wave erosion, M_e. This suggests that the overall iceberg evolution will be sensitive to the choice of representation of M_e. The form given in equation (4) is adapted from *Bigg et al.* [1997], using the representation of the sea state in *Martin and Adcroft* [2010] and assuming $|\vec{v}_a| \gg |\vec{v}_i|$. *Gladstone et al.* [2001] (henceforth G01) introduce sea ice and SST dependences to this term, $M_e = M_0 \left(p_1 + p_2 T_w\right) \left[1 + \cos\left(C^3 \pi\right)\right]/2$, where M_0 is the form of M_e given in equation (4), $p_1 = 0.67$, $p_2 = 0.33$ °C^{-1}, and C is the sea ice concentration. *Jongma et al.* [2009] (henceforth J09), on the other hand, use a form that is independent of SST but has a different representation of the sea state, which leads to $M_e = q_1 + \sqrt{q_2 + q_3 |\vec{v}_a|}$, where $q_1 = -2.9 \times 10^{-5}$ m/s, $q_2 = 1.1 \times 10^{-9}$ m^2/s^2, and $q_3 = 2.4 \times 10^{-10}$ m/s. These three formulations have each been used in a number of subsequent studies.

In what follows we will focus on simulations with a representation of M_e as in equation (4), but we will also perform two further sets of simulations that instead use the G01 or J09 representations. This will allow us to assess the impact of the choice of M_e representation on the iceberg trajectories and meltwater distribution. Since iceberg release locations are chosen to be near the winter sea ice edge (see below), we will take sea ice concentration, C, to be zero for all simulations.

2.3. Simulated Iceberg Trajectories and Freshwater Flux

We consider 10 initial iceberg size classes, with dimensions ranging from 100 × 67 × 67 m (class 1) to 1500 × 1000 × 300 m (class 10), similar to the classification of *Bigg et al.* [1997]. The iceberg dimensions for all initial size classes are given in Table S1. One thousand icebergs of each size (10^4 icebergs in total) are released in the North Atlantic during the course of the study period. The icebergs move as Lagrangian particles following the precomputed circulation fields.

For the purpose of the present study, we choose iceberg release locations in Baffin Bay, near the southern tip of Baffin Island (red square in Figure 1, centered at 62°N, 62°W). This location allows us to directly test the impact of the differences in ocean and atmosphere conditions between the ECCO2 and CCSM4 simulations, although it is somewhat farther southwest than the origin of most modern-day icebergs.

The resulting iceberg drift behavior is illustrated with 25 sample trajectories for each of the five size classes in Figures 1a–1b. The freshwater entering the ocean from iceberg melt, F, is computed from the rate of change in iceberg volume, dV/dt, such that $F(\vec{x}_i, t) = (\rho_i/\rho_w)(dV/dt)$, where $\vec{x}_i(t)$ is the position along a given iceberg trajectory. The freshwater flux is F divided by the grid box area. Figures 1c–1e show the spatial distribution of total freshwater flux for ECCO2 and CCSM4, as well as the difference. These are obtained by first computing the freshwater flux per 100 km^3 of initial iceberg volume for each iceberg size class. We then sum over all classes, weighing each class according to the empirically based lognormal distribution of *Bigg et al.* [1997], which assigns more weight to smaller icebergs that are observed to occur more frequently. Freshwater fluxes from the individual size classes 1, 5, and 10 are shown in Figure S2. Figure 1 is computed using the representation of M_e given in equation (4). Corresponding results for the G01 and J09 representations are shown in Figures S3 and S4.

3. Differences in Freshwater Flux and Surface Conditions

The freshwater distributions of ECCO2 and CCSM4 exhibit some expected similarities and striking differences. Both distributions clearly show that the icebergs are strongly advected by the western boundary current, i.e.,

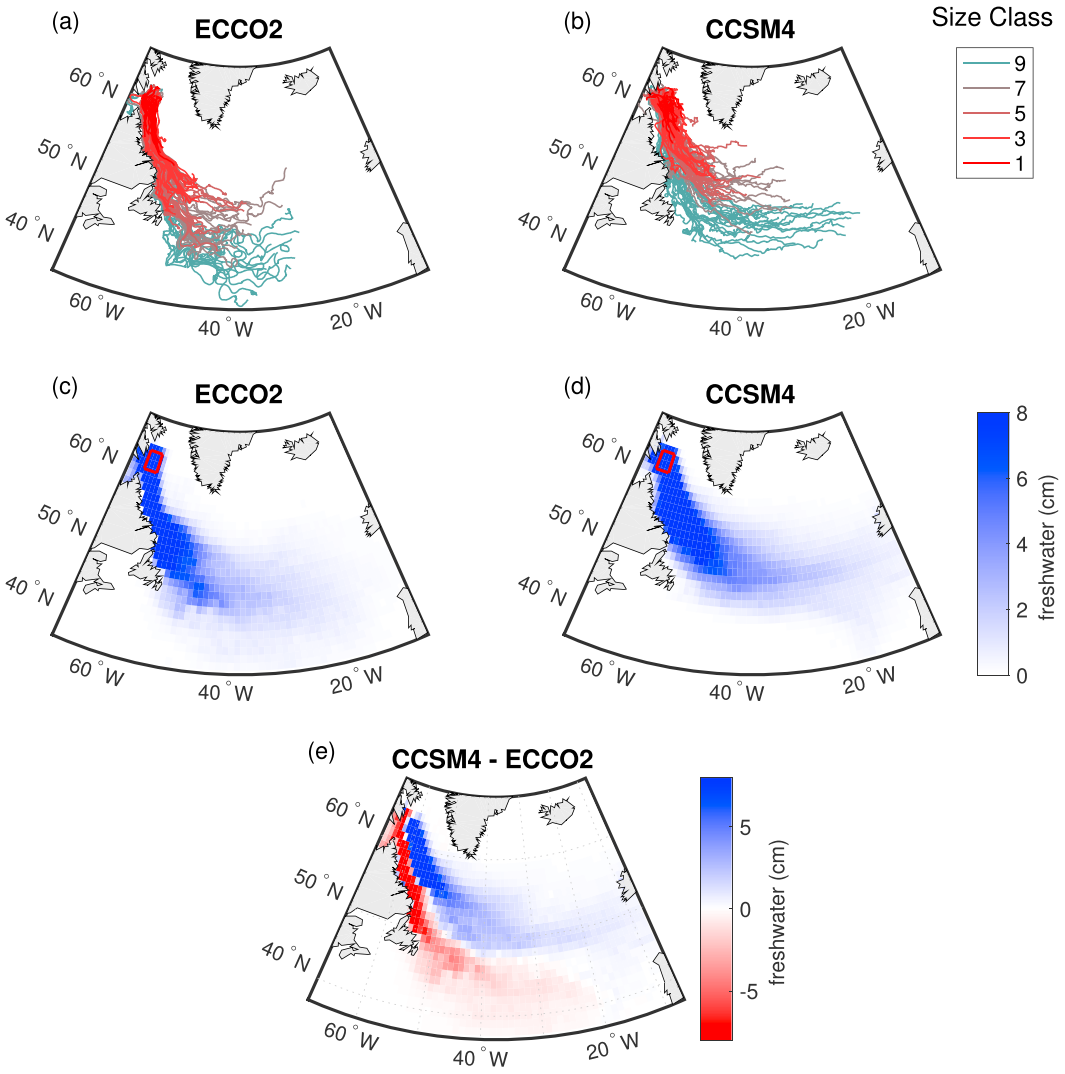

Figure 1. Trajectories and total freshwater flux from iceberg melt. Shown are 25 iceberg trajectories simulated using (a) ECCO2 output fields or (b) CCSM4 output fields for five different size classes (color coded as indicated in the figure legend). (c) Time-integrated ECCO2 freshwater flux per km^3 of iceberg volume released; the red square indicates the iceberg seeding region. (d) As in Figure 1a but for CCSM4. (e) Difference in freshwater distribution between CCSM4 and ECCO2, with red shading indicating more ECCO2 flux and blue shading indicating more CCSM4 flux.

the Labrador Current that flows from Baffin Island southward toward Newfoundland. The most noticeable difference between the two simulations is that ECCO2 icebergs stay closer to the coast and reach more southern latitudes than their CCSM4 counterparts, which remain in more northern and eastern regions.

Figures S3 and S4 illustrate that the differences between the ECCO2 and CCSM4 simulations are similar for all three representations of M_e, with CCSM4 freshwater being consistently confined to more northern and eastern regions. The G01 M_e rates are on average somewhat higher than those simulated with J09 and equation (4), and they have a more pronounced seasonal cycle due to their explicit SST dependence.

The remainder of this study focuses on explaining the differences between the ECCO2 and CCSM4 simulations. We do so by considering first the mean oceanic and atmospheric surface conditions and then how these conditions impact the iceberg evolution.

Figure 2 shows the 1992–2005 time-averaged North Atlantic surface water and air speeds, velocity vector fields, and SSTs, for ECCO2 and CCSM4. The most pronounced difference in the circulation fields is that wind speeds are considerably higher in CCSM4 than in the atmospheric reanalysis forcing used in ECCO2. This is

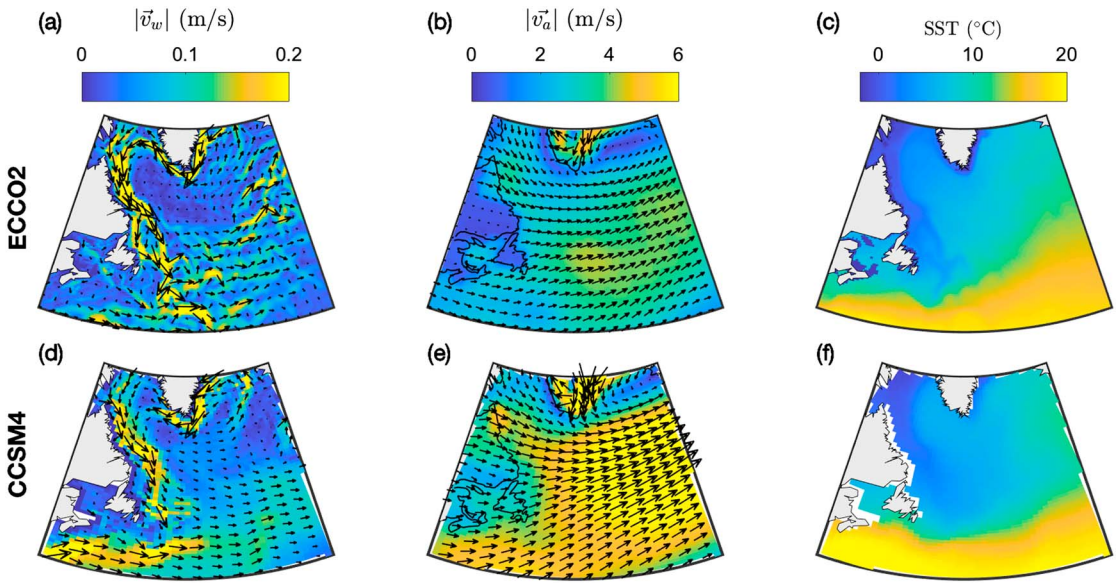

Figure 2. Time-averaged circulation and SST conditions in the model runs. (a–c) ECCO2 and (d–f) CCSM4. Figures 2a and 2d show surface current velocity (arrows) and speed (shading). Figures 2b and 2e show surface wind velocity (arrows) and speed (shading). Figures 2c and 2f show SST.

qualitatively representative of the suite of GCMs from CMIP5, which tend to simulate midlatitude westerlies that are too strong compared to observational estimates [*Flato et al.*, 2013; *Lee et al.*, 2013]. We find that average wind speeds experienced by CCSM4 and ECCO2 icebergs are $\langle|\vec{v}_a|\rangle = 9.5 \pm 0.6$ m/s and 5.4 ± 0.4 m/s, respectively (averaged over all trajectories and all size classes, with uncertainties representing 1 standard deviation). This difference is largely due to the zonal component, which is on average almost twice as high in CCSM4.

The differences in the ocean current velocities are comparatively minor, with CCSM4 simulating the western boundary currents near Greenland and Labrador in reasonably good agreement with ECCO2. The higher-resolution ECCO2 output, however, does feature somewhat higher speeds in these boundary currents, with the average water speed experienced by ECCO2 icebergs being $\langle|\vec{v}_w|\rangle = 0.13 \pm 0.03$ m/s compared with $\langle|\vec{v}_w|\rangle = 0.09 \pm 0.02$ m/s for CCSM4 icebergs.

One might expect that the bias toward stronger westerlies in CCSM4 would lead to a greater spread of iceberg meltwater. However, the opposite occurs: despite much weaker winds, ECCO2 icebergs travel on average slightly farther than CCSM4 icebergs for all except the two largest size classes (Figure 3a). We find that this somewhat counterintuitive result can be attributed to two effects: (i) the tendency toward enhanced meltwater spread due to the faster iceberg drift in CCSM4 being largely compensated by faster wind-driven wave erosion and (ii) the faster-flowing Labrador Current in ECCO2, which advects icebergs more rapidly southward close to the coast.

Before examining these two effects in more detail, we briefly consider the differences in the time-averaged SST fields (Figures 2c and 2f). Both temperature fields indicate a cold southward surface transport associated with the Labrador Current. SSTs in CCSM4 are colder for most of the region north of the Grand Banks (~47°N). Average SSTs experienced by icebergs of size class 10 are 6.4°C in ECCO2 and 8.0°C in CCSM4. The differences are smaller along trajectories of smaller icebergs, and the average SST for size class 1 icebergs is approximately 0.6°C in both ECCO2 and CCSM4. However, even for size class 10, the average thermal erosion is just $\langle M_v \rangle \lesssim 0.5$ m/d in both sets of simulations. This is nearly an order of magnitude smaller than the wind-driven wave erosion (described below), so it has relatively little impact on the large-scale meltwater distribution.

4. Impacts of Model Biases in Surface Winds and Boundary Currents

Surface wind velocities play an important role in the distribution of iceberg meltwater, since they are dominant drivers of both iceberg motion and iceberg ablation. These two processes have opposing effects on the spread of meltwater: while faster drift due to stronger winds spreads meltwater further, the faster wave erosion due to stronger winds acts to reduce the spread of meltwater.

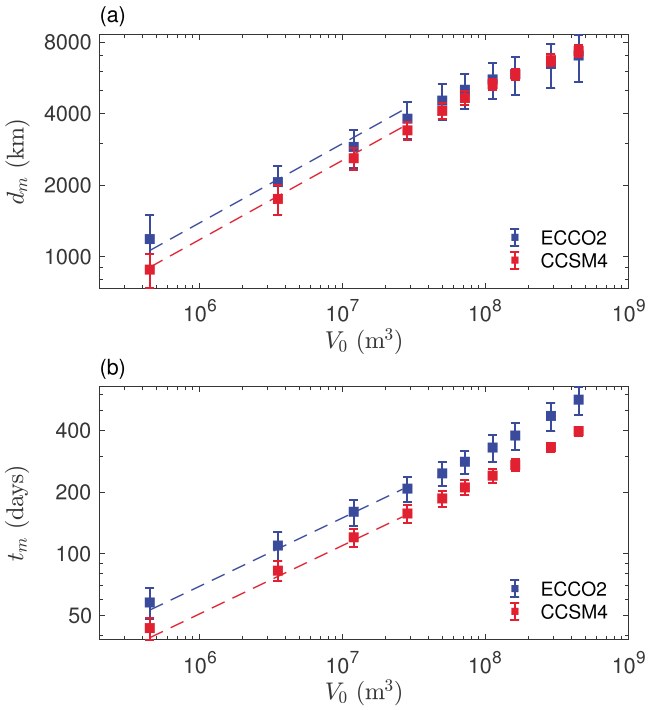

Figure 3. Iceberg trajectory lengths and life spans in ECCO2 and CCSM4 simulations. (a) Total distance traveled by icebergs at the time of final melt, d_m, showing that ECCO2 icebergs (blue) travel farther than CCSM4 icebergs (red) for most size classes. Each square shows the average over all trajectories for one initial size class, and error bars indicate 1 standard deviation. The dashed lines correspond to the analytic approximation given by equation (6), which approximately holds for size classes 1–4. (b) Time of final melt, t_m, for each size class, showing that ECCO2 icebergs live longer than CCSM4 icebergs. The dashed lines correspond to the analytic approximation given by equation (7).

For the average wind speeds given in section 3, we find that the average wind-driven wave erosion, $\langle M_e \rangle$, is 3.0 m/d for CCSM4 and 2.2 m/d for ECCO2. Wave erosion is the dominant decay process, making up ~70% of the total ablation in both CCSM4 and ECCO2.

We can estimate whether higher winds lead to more meltwater spread due to drift or less meltwater spread due to wave erosion by analytically solving a simplified version of the model (1)–(4). We consider an iceberg subject only to wind-driven motion, with $\vec{v}_w = 0$. Focusing on the distance traveled but not the direction, we examine the magnitude of the iceberg velocity. In this case equation (1) becomes

$$|\vec{v}_i| = \gamma\sqrt{\alpha^2+\beta^2}|\vec{v}_a| = \gamma\frac{\sqrt{\sqrt{1+4\Lambda^4}-1}}{\sqrt{2}\Lambda}|\vec{v}_a|$$

using the expression (3) for α and β. Note that Λ depends on the wind speed and iceberg size. However, for large $|\vec{v}_a|$, this reduces to

$$|\vec{v}_i| \approx \gamma|\vec{v}_a|. \tag{5}$$

This approximation is accurate to within 10% when $|\vec{v}_a| \gtrsim 1$ m/s for size class 1 and $|\vec{v}_a| \gtrsim 20$ m/s for size class 10. The average wind speed experienced by the simulated icebergs is 5–10 m/s, making equation (5) a rather crude scaling for larger icebergs.

The iceberg speed can be integrated to obtain the total length of the trajectory,

$$d_m = \int_0^{t_m} |\vec{v}_i| \mathrm{d}t \approx \gamma|\vec{v}_a| t_m, \tag{6}$$

where t_m is the time of complete melt. Here we have used the approximation (5) and assumed $|\vec{v}_a|$ to be constant.

Considering ablation from wave erosion alone (i.e., $M_b = M_v = 0$), and adopting the initial length-to-width ratio of $L_0/W_0 = 1.5$, which has been widely used in previous iceberg modeling studies [e.g., *Bigg et al.*, 1997] and adopted in this study (Table S1), it can then be shown that

$$t_m = rW_0/M_e, \tag{7}$$

where the factor r is due to iceberg capsizing [*Wagner et al.*, 2017]. For $W_0 = H_0$, as is the case for size classes 1–4, $r = 1.75$ [*Wagner et al.*, 2017]. Inserting the expression (4) for M_e, this allows us to estimate the length of the iceberg trajectory (6) as a function of wind speed and initial iceberg width, giving

$$d_m \approx \gamma r W_0 \frac{|\vec{v}_a|}{M_e} = \gamma r W_0 \frac{|\vec{v}_a|}{a_1\sqrt{|\vec{v}_a|}+a_2|\vec{v}_a|}. \tag{8}$$

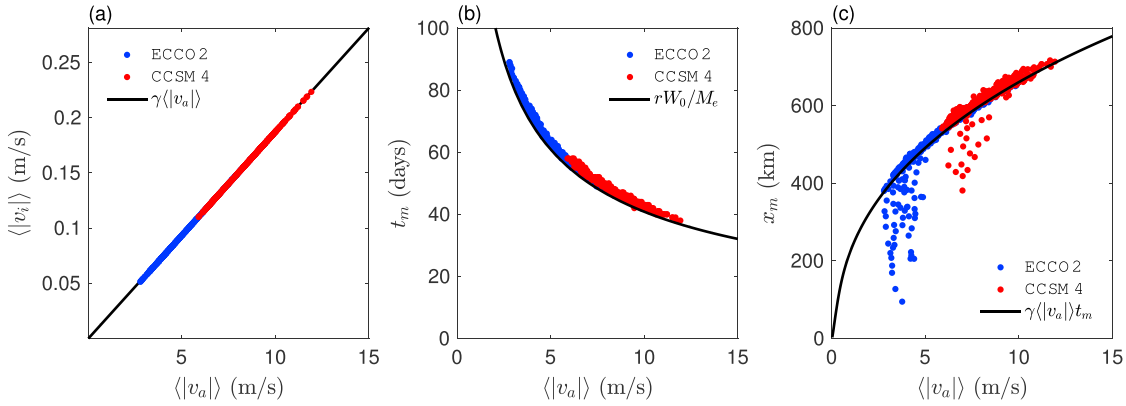

Figure 4. Iceberg characteristics versus average wind speeds in the wind-only model runs using size class 1. (a) Mean iceberg speeds, $\langle|\vec{v}_i|\rangle$, versus mean wind speeds $\langle|\vec{v}_a|\rangle$. Each dot corresponds to the along-track average of one individual iceberg trajectory, and 500 trajectories are shown. ECCO2 and CCSM4 icebergs are shown in blue and red, respectively. The analytical approximation (5) is shown in black. (b) Iceberg life span, t_m, versus $\langle|\vec{v}_a|\rangle$, with the approximation (7) in black. (c) Total distance traveled for each iceberg, d_m, versus $\langle|\vec{v}_a|\rangle$, with the approximation (8) in black. Simulated icebergs that most substantially do not match the black curve have spent prolonged periods grounded in shallow waters, which reduces their total distance traveled and is not accounted for in the analytical approximation.

This implies that for relatively small $|\vec{v}_a|$ (but still large enough to allow the approximation in (equation 5)), $d_m \approx \gamma r W_0 \sqrt{|\vec{v}_a|}/a_1$, whereas in the limit of large $|\vec{v}_a|$, $d_m = \gamma r W_0/a_2$. In other words, the effect of drift dominates over wave erosion for relatively slow wind speeds and $d_m \sim \sqrt{|\vec{v}_a|}$, whereas the drift and wave erosion effects exactly compensate for very large wind speeds such that d_m is independent of $|\vec{v}_a|$.

We evaluate the accuracy of this approximate analysis using a set of "wind-only" simulations in which we set $\vec{v}_w = 0$ in the full model. Figure 4 illustrates the case for size class 1 icebergs, and it indicates that equations (7) and (8) provide reasonably accurate approximations for small icebergs. These approximations become less accurate for larger icebergs (Figures S5 and S6). Note that the results are similar when considering the linear distance between iceberg release location and location of final melt, rather than the length of the trajectory.

The wind-only simulations illustrate that the higher wind speeds in CCSM4 (Figure 4a) cause the icebergs to travel farther (Figure 4c), although this effect is diminished through faster melt leading to shorter CCSM4 iceberg life spans (Figure 4b). Note that all size classes have a shorter life span in CCSM4 when ocean currents are included (Figure 3b). The fact that CCSM4 icebergs travel farther than ECCO2 in the wind-only simulations (Figure 4c) but less far in the simulations that include ocean currents (Figure 3a) supports the conclusion that it is the ocean currents that cause the greater spread of ECCO2 icebergs.

This conclusion is further supported by the results in Figure 5, which is similar to Figure 4 but includes ocean currents. In Figure 5a, the relationship between $\langle|\vec{v}_i|\rangle$ and $\langle|\vec{v}_a|\rangle$ is similar to Figure 4a among the CCSM4 icebergs and among the ECCO2 icebergs, although the correlations are much lower due to the influence of ocean currents (Pearson correlation coefficients are given in the figure). Indeed, there is a similar relationship between $\langle|\vec{v}_i|\rangle$ and $\langle|\vec{v}_w|\rangle$ (Figure 5d), with similar correlation coefficients. However, ECCO2 water speeds are noticeably faster than in CCSM4, in contrast to the air speeds which are faster in CCSM4.

Figure 5 illustrates that winds and ocean currents have opposing effects on icebergs in two respects:

1. The iceberg life span is strongly dependent on the wind speeds (Figure 5b), just as in the wind-only scenario, and even here it is closely approximated by the analytical solution (7). The water velocities, by contrast, do not affect ablation substantially, as illustrated by the low correlation between t_m and $\langle|\vec{v}_w|\rangle$ in Figure 5e.
2. The competing wind-driven wave erosion and drift processes lead to a weaker dependence of the total distance traveled, d_m, on the wind speeds (Figure 5c). The strong western boundary currents, on the other hand, cause d_m to be highly correlated with the ocean current speeds, $\langle|\vec{v}_w|\rangle$ (Figure 5f).

The dashed lines in Figures 5a and 5d indicate very rough approximations to these relations. They were made by approximating the magnitude of the ice speed by the linear addition of the magnitudes of the air and water terms in equation (1) and also incorporating the large Λ approximation that was used in equation (5), such that $|\vec{v}_i| \approx |\vec{v}_w| + \gamma|\vec{v}_a|$. Similarly, the dashed lines in Figures 5c and 5f are found by multiplying the

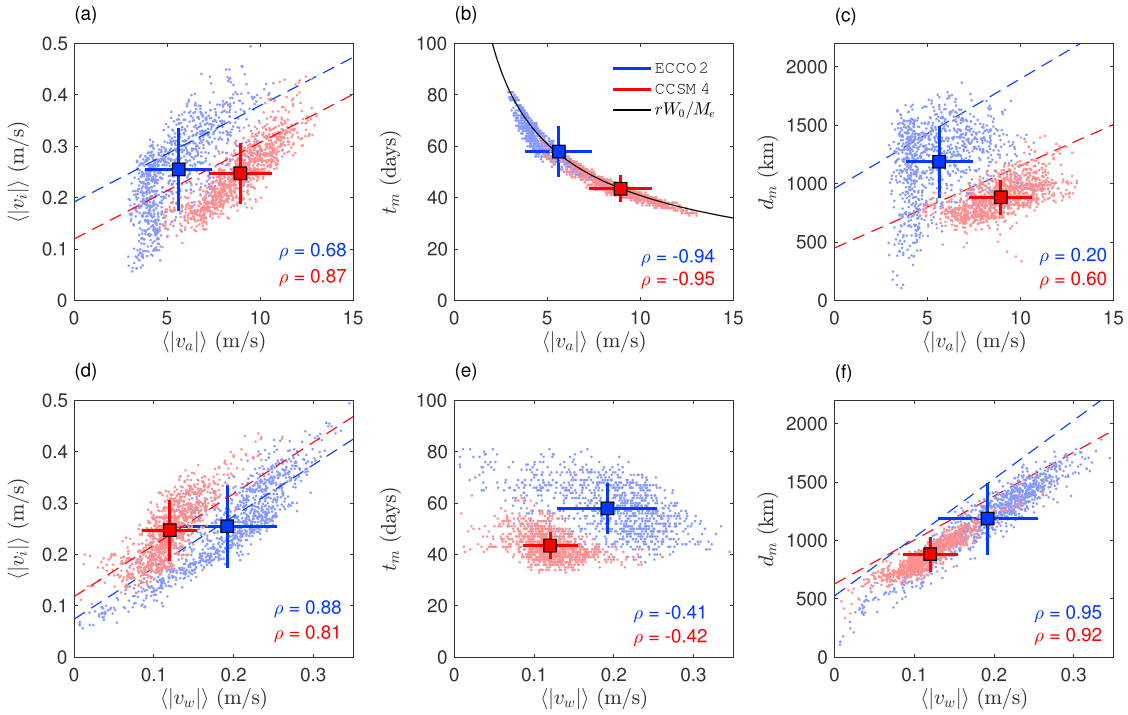

Figure 5. Iceberg characteristics versus average wind and ocean current speeds for size class 1. (a–c) As in Figure 4 but for output from the full model runs that include ocean currents. (d–f) The same iceberg characteristics as Figures 5a–5c but plotted against $\langle|\vec{v}_w|\rangle$. In addition to the average values for each individual trajectory (points), we also show the average over all trajectories (squares), with error bars indicating 1 standard deviation. Dashed lines show analytical approximations (see text). Pearson's correlation coefficients (ρ) are given for ECCO2 (blue) and CCSM4 (red).

approximated $|\vec{v}_i|$ by the simulated mean iceberg life span, $d_m \approx \left(|\vec{v}_w| + \gamma|\vec{v}_a|\right) t_m$. These roughly correspond to upper limits on $|\vec{v}_i|$ and d_m, since the air and water drag terms in equation (1) typically point in different directions (which causes the magnitude of their sum to be smaller than the sum of their magnitudes). Overall, Figure 5 highlights that localized model biases in the ocean currents can have a strong impact on the large-scale distribution of iceberg meltwater.

5. Conclusions

In summary, we find that the release of iceberg meltwater based on the CCSM4 simulated surface ocean and atmosphere conditions is limited to a region that is too far north and east, compared with the meltwater release from the ECCO2 observational state estimate. The smaller spread of the CCSM4 icebergs is primarily a consequence of localized biases toward slower simulated ocean currents in the GCM, which may be linked to factors including insufficient horizontal model resolution. This is noteworthy because the differences between the ECCO2 and CCSM4 wind fields are much more visually striking than the differences between the ocean current fields. Furthermore, *Wagner et al.* [2016] recently found that the wind contribution to iceberg drift (final term in equation (1)) is substantial and can dominate that of the ocean by up to a factor of 3 (in the limit of small icebergs). The muted impact of the large wind bias on the spread of meltwater can be attributed to compensation between faster winds causing farther iceberg drift and also more rapid iceberg ablation.

These results may have consequences for the simulation of the Atlantic meridional overturning circulation (AMOC), which has been projected to slow down under increased future freshwater input from Greenland [*Lenaerts et al.*, 2015]. Furthermore, these findings may inform simulations of the Heinrich events during the last glacial period, which are believed to have involved large discharges of icebergs into the North Atlantic and a slowdown of the AMOC [e.g., *Hemming*, 2004; *McManus et al.*, 2004]. Since calving fluxes from Greenland are predicted to increase under rising global temperatures, an accurate representation of freshwater release from icebergs may be important for climate projections. The findings in this study suggest that while the survival of North Atlantic icebergs is likely curtailed by the high bias in GCM surface winds, the distribution of iceberg meltwater may depend crucially on relatively small scale features of ocean surface currents.

Acknowledgments
The authors thank Rebecca W. Dell for her contribution to the model development and Navid Constantinou for helpful discussions. Two anonymous reviewers are acknowledged for their highly constructive comments. This work was supported by ONR grant N00014-13-1-0469 and National Science Foundation grant OCE-1357078. The code to integrate the iceberg drift and decay model is available at http://eisenman.ucsd.edu/code.html.

References

Bigg, G. R., M. R. Wadley, D. P. Stevens, and J. A. Johnson (1997), Modelling the dynamics and thermodynamics of icebergs, *Cold Reg. Sci. Technol.*, *26*(2), 113–135.

Bügelmayer, M., D. M. Roche, and H. Renssen (2015), How do icebergs affect the Greenland ice sheet under pre-industrial conditions? — A model study with a fully coupled ice-sheet-climate model, *Cryosphere*, *9*(3), 821–835.

Depoorter, M. A., J. L. Bamber, J. A. Griggs, J. T. M. Lenaerts, S. R. M. Ligtenberg, M. R. van den Broeke, and G. Moholdt (2013), Calving fluxes and basal melt rates of Antarctic ice shelves, *Nature*, *502*(7469), 89–92.

Duprat, L. P. A. M., G. R. Bigg, and D. J. Wilton (2016), Enhanced Southern Ocean marine productivity due to fertilization by giant icebergs, *Nat. Geosci.*, *9*(3), 219–221.

Enderlin, E. M., I. M. Howat, S. Jeong, M. J. Noh, J. H. Angelen, and M. R. Broeke (2014), An improved mass budget for the Greenland ice sheet, *Geophys. Res. Lett.*, *41*, 866–872, doi:10.1002/2013GL059010.

Flato, G., et al. (2013), Evaluation of climate models, in *Climate Change 2013: The Physical Science Basis. Contribution of Working Group I to the Fifth Assessment Report of the Intergovernmental Panel on Climate Change*, pp. 741–866, Cambridge Univ. Press, Cambridge.

Gent, P. R., et al. (2011), The Community Climate System Model Version 4, *J. Clim.*, *24*(19), 4973–4991.

Gladstone, R. M., G. R. Bigg, and K. W. Nicholls (2001), Iceberg trajectory modeling and meltwater injection in the Southern Ocean, *J. Geophys. Res.*, *106*(C9), 19,903–19,915.

Hemming, S. R. (2004), Heinrich events: Massive late Pleistocene detritus layers of the North Atlantic and their global climate imprint, *Rev. Geophys.*, *42*, RG1005, doi:10.1029/2003RG000128.

Hunke, E. C., and D. Comeau (2011), Sea ice and iceberg dynamic interaction, *J. Geophys. Res.*, *116*, C05008, doi:10.1029/2010JC006588.

Jongma, J. I., E. Driesschaert, T. Fichefet, H. Goosse, and H. Renssen (2009), The effect of dynamic-thermodynamic icebergs on the Southern Ocean climate in a three-dimensional model, *Ocean Modell.*, *26*(1–2), 104–113.

Jongma, J. I., H. Renssen, and D. M. Roche (2013), Simulating Heinrich event 1 with interactive icebergs, *Clim. Dyn.*, *40*(5–6), 1373–1385.

Joughin, I., B. E. Smith, and B. Medley (2014), Marine ice sheet collapse potentially under way for the Thwaites Glacier Basin, West Antarctica, *Science*, *344*(6185), 735–738.

Lee, T., D. E. Waliser, J.-L. F. Li, F. W. Landerer, and M. M. Gierach (2013), Evaluation of CMIP3 and CMIP5 wind stress climatology using satellite measurements and atmospheric reanalysis products, *J. Clim.*, *26*(16), 5810–5826.

Lenaerts, J. T. M., D. Le Bars, L. van Kampenhout, M. Vizcaino, E. M. Enderlin, and M. R. van den Broeke (2015), Representing Greenland ice sheet freshwater fluxes in climate models, *Geophys. Res. Lett.*, *42*, 6373–6381, doi:10.1002/2015GL064738.

Liu, Y., J. C. Moore, X. Cheng, R. M. Gladstone, J. N. Bassis, H. Liu, J. Wen, and F. Hui (2015), Ocean-driven thinning enhances iceberg calving and retreat of Antarctic ice shelves, *Proc. Natl. Acad. Sci. U.S.A.*, *112*(11), 3263–3268.

Marsh, R., et al. (2015), NEMO-ICB (v1.0): Interactive icebergs in the NEMO ocean model globally configured at eddy-permitting resolution, *Geosci. Model Dev.*, *8*(5), 1547–1562.

Martin, T., and A. Adcroft (2010), Parameterizing the fresh-water flux from land ice to ocean with interactive icebergs in a coupled climate model, *Ocean Modell.*, *34*(3–4), 111–124.

McManus, J. F., R. Francois, J. M. Gherardi, L. D. Keigwin, and S. Brown-Leger (2004), Collapse and rapid resumption of Atlantic meridional circulation linked to deglacial climate changes, *Nature*, *428*(6985), 834–837.

Menemenlis, D., J. M. Campin, and P. Heimbach (2008), ECCO2: High resolution global ocean and sea ice data synthesis, *Mercator Ocean Q. Newsletter*, *31*, 13–21.

Merino, N., J. Le Sommer, G. Durand, N. C. Jourdain, G. Madec, P. Mathiot, and J. Tournadre (2016), Antarctic icebergs melt over the Southern Ocean: Climatology and impact on sea ice, *Ocean Modell.*, *104*, 99–110.

Onogi, K., et al. (2007), The JRA-25 reanalysis, *J. Meteorol. Soc. Jpn.*, *85*(3), 369–432.

Rignot, E., I. Velicogna, M. R. van den Broeke, A. Monaghan, and J. Lenaerts (2011), Acceleration of the contribution of the Greenland and Antarctic ice sheets to sea level rise, *Geophys. Res. Lett.*, *38*, L05503, doi:10.1029/2011GL046583.

Roberts, W. H. G., P. J. Valdes, and A. J. Payne (2014), A new constraint on the size of Heinrich Events from an iceberg/sediment model, *Earth Planet. Sci. Lett.*, *386*, 1–9.

Sierro, F. J., et al. (2005), Impact of iceberg melting on Mediterranean thermohaline circulation during Heinrich events, *Paleoceanography*, *20*, PA2019, doi:10.1029/2004PA001051.

Smith, K. L. J., A. D. Sherman, T. J. Shaw, and J. Sprintall (2013), Icebergs as unique Lagrangian ecosystems in polar seas, *Annu. Rev. Mar. Sci.*, *5*(1), 269–287.

Stern, A. A., et al. (2015), Wind-driven upwelling around grounded tabular icebergs, *J. Geophys. Res. Oceans*, *120*(8), 5820–5835, doi:10.1002/2015JC010805.

Stern, A. A., A. Adcroft, and O. Sergienko (2016), The effects of Antarctic iceberg calving-size distribution in a global climate model, *J. Geophys. Res. Oceans*, *121*, 5773–5788, doi:10.1002/2016JC011835.

Taylor, K. E., R. J. Stouffer, and G. A. Meehl (2012), An overview of CMIP5 and the experiment design, *Bull. Am. Meteorol. Soc.*, *93*(4), 485–498.

van den Berk, J., and S. S. Drijfhout (2014), A realistic freshwater forcing protocol for ocean-coupled climate models, *Ocean Modell.*, *81*, 36–48.

Vernet, M., et al. (2012), Islands of ice: Influence of free-drifting Antarctic icebergs on pelagic marine ecosystems, *Oceanography*, *25*(3), 38–39.

Wagner, T. J. W., R. W. Dell, and I. Eisenman (2016), An analytical model of iceberg drift, arXiv:1610.06403.

Wagner, T. J. W., A. A. Stern, R. W. Dell, and I. Eisenman (2017), Representing the rolling of icebergs in climate models, arXiv:1702.06870.

Weeks, W. F., and M. Mellor (1978), Some elements of iceberg technology, *Tech. Rep.*, Cold Reg. Res. and Eng. Lab.

Supporting Information for "How climate model biases skew the distribution of iceberg meltwater"

Till J.W. Wagner[1] and Ian Eisenman[1]

Contents of this file

1. Table S1
2. Figures S1 to S6

[1]Scripps Institution of Oceanography, University of California San Diego, USA

0094-8276/17/$5.00

Size Class	L_0 (m)	$W_0(m)$	H_0 (m)	$\epsilon_0 = W_0/H_0$
1	100	67	67	1
2	200	133	133	1
3	300	200	200	1
4	400	267	267	1
5	500	333	300	1.11
6	600	400	300	1.33
7	750	500	300	1.67
8	900	600	300	2
9	1200	800	300	2.67
10	1500	1000	300	3.33

Table 1. Initial iceberg dimensions for the 10 size classes used here [adapted from Bigg *et al.* (1997)].

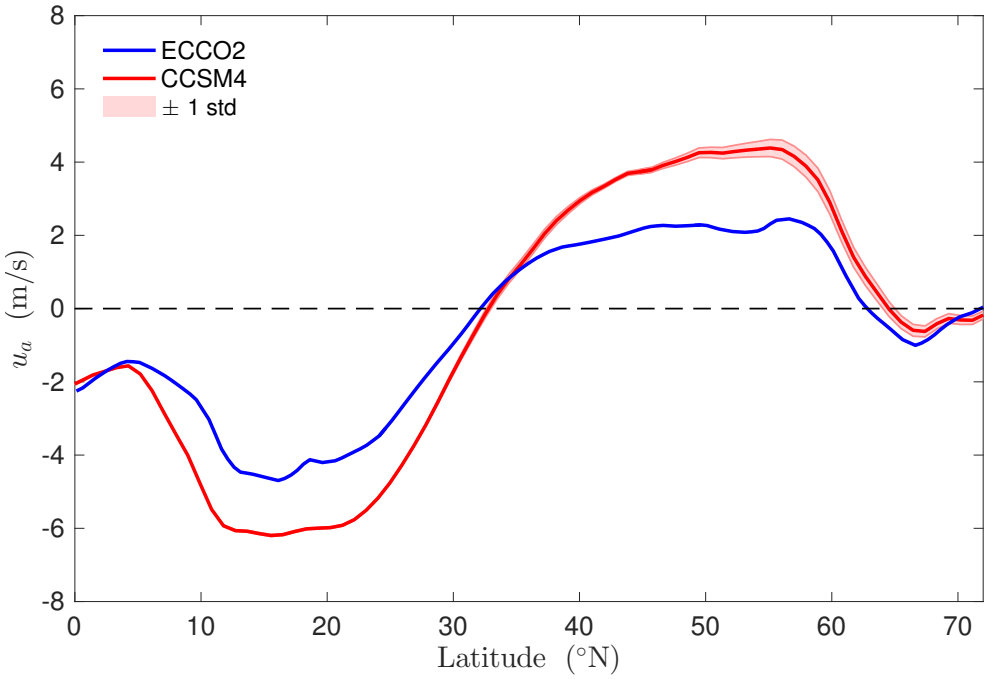

Figure S1. Zonal-mean zonal surface wind velocity in CCSM4 (red) and ECCO2 (blue) averaged over the study period 1992-2005. The red line represents the ensemble mean of the 6 CCSM4 runs and red shading indicates the spread among the ensemble members. The individual CCSM4 runs differ only in their initial conditions and hence represent different realizations of internal variability. The narrow range of the shading indicates that internal variability has little influence on these 14-year means.

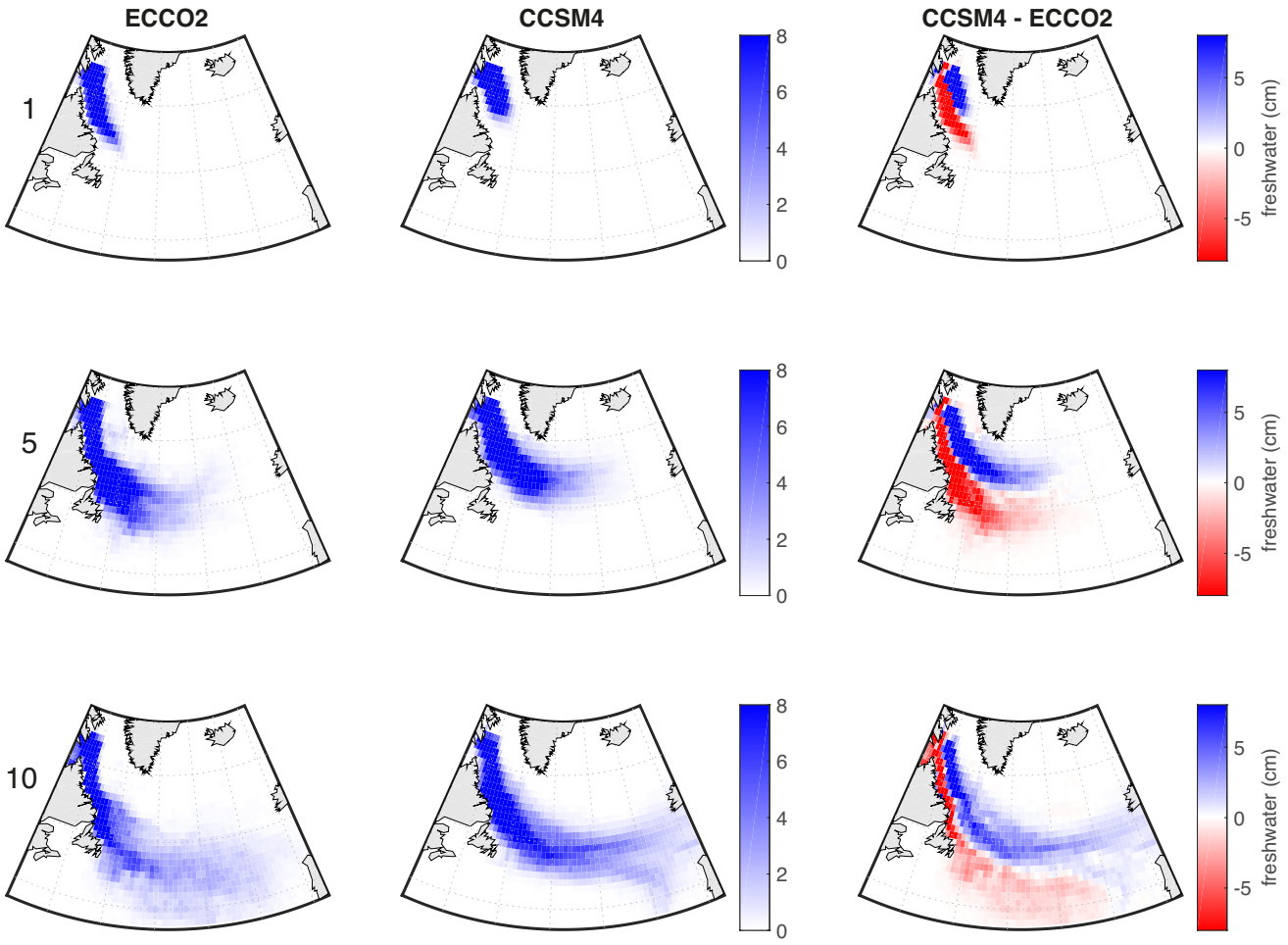

Figure S2. Freshwater flux from iceberg melt for iceberg size class 1 (top row), iceberg size class 5 (middle row), and iceberg size class 10 (bottom row). Shown are simulations using the ECCO2 output fields (left column), the CCSM4 output fields (center column), and the difference between the two (right column).

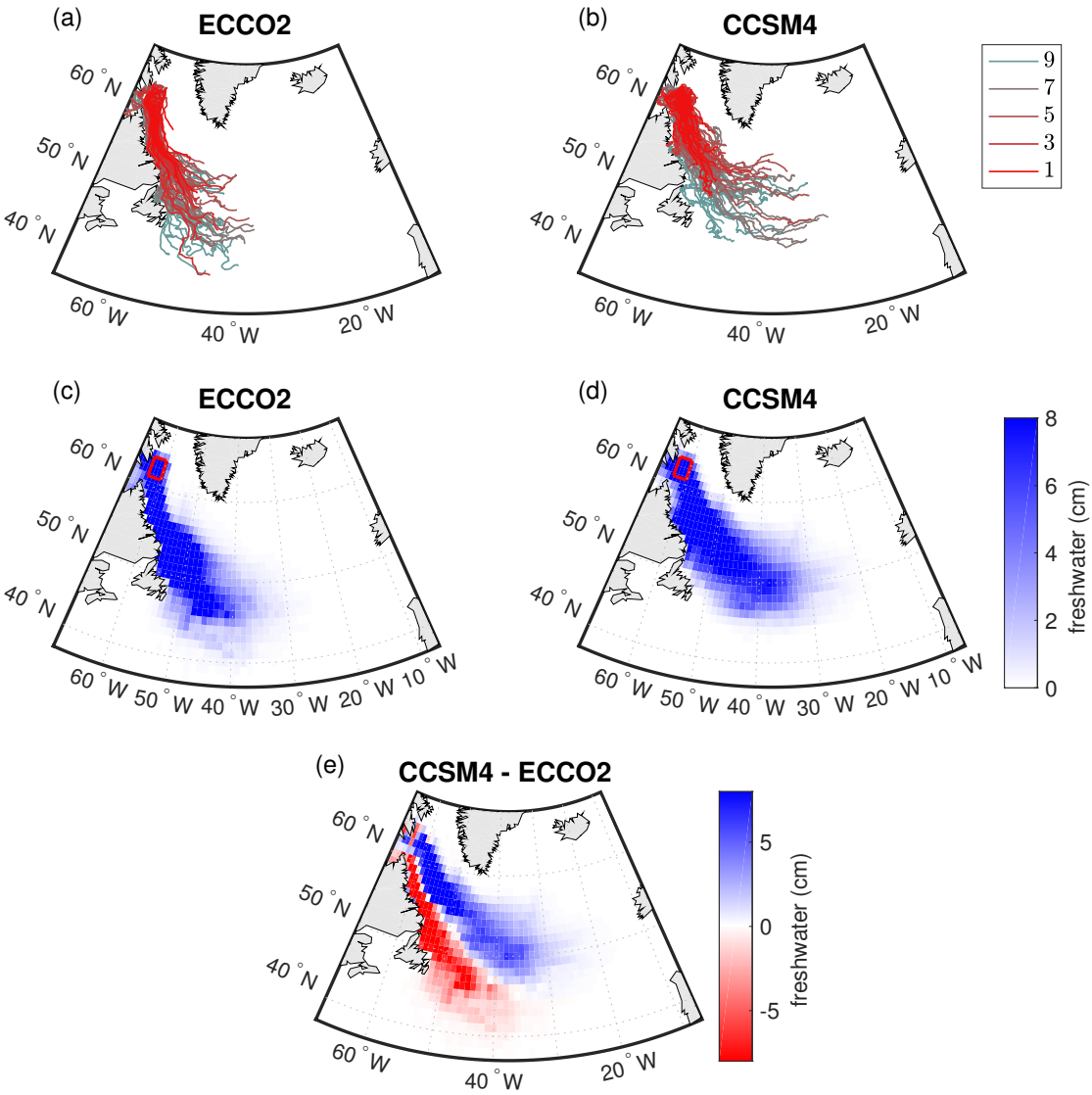

Figure S3. As Fig. 1 in the main text, but using the representation of M_e from G01. Note that to obtain M_e in equation (4) in the main text, we take the formulation of wave erosion given by Bigg et al. (1997), $M_e = S_s/2$, where S_s is the sea state and M_e is in m/d. Martin & Adcroft (2010) represent the sea state as $S_s = \frac{3}{2}|\vec{v}_a - \vec{v}_w|^{1/2} + \frac{1}{10}|\vec{v}_a - \vec{v}_w|$, which we adopt in this study. We rewrite this with dimensional parameters in equation (4). In G01, the wind-driven wave erosion term is written as $M_e = \frac{1}{12} S_s (T_w + 2)\,[1 + \cos(\,C^3\pi\,)]$, where S_s is the sea state and M_e is in m/d. G01 do not provide an explicit expression for S_s, and we use the representation from Martin & Adcroft (2010) to arrive at the G01 equation for M_e in the main text.

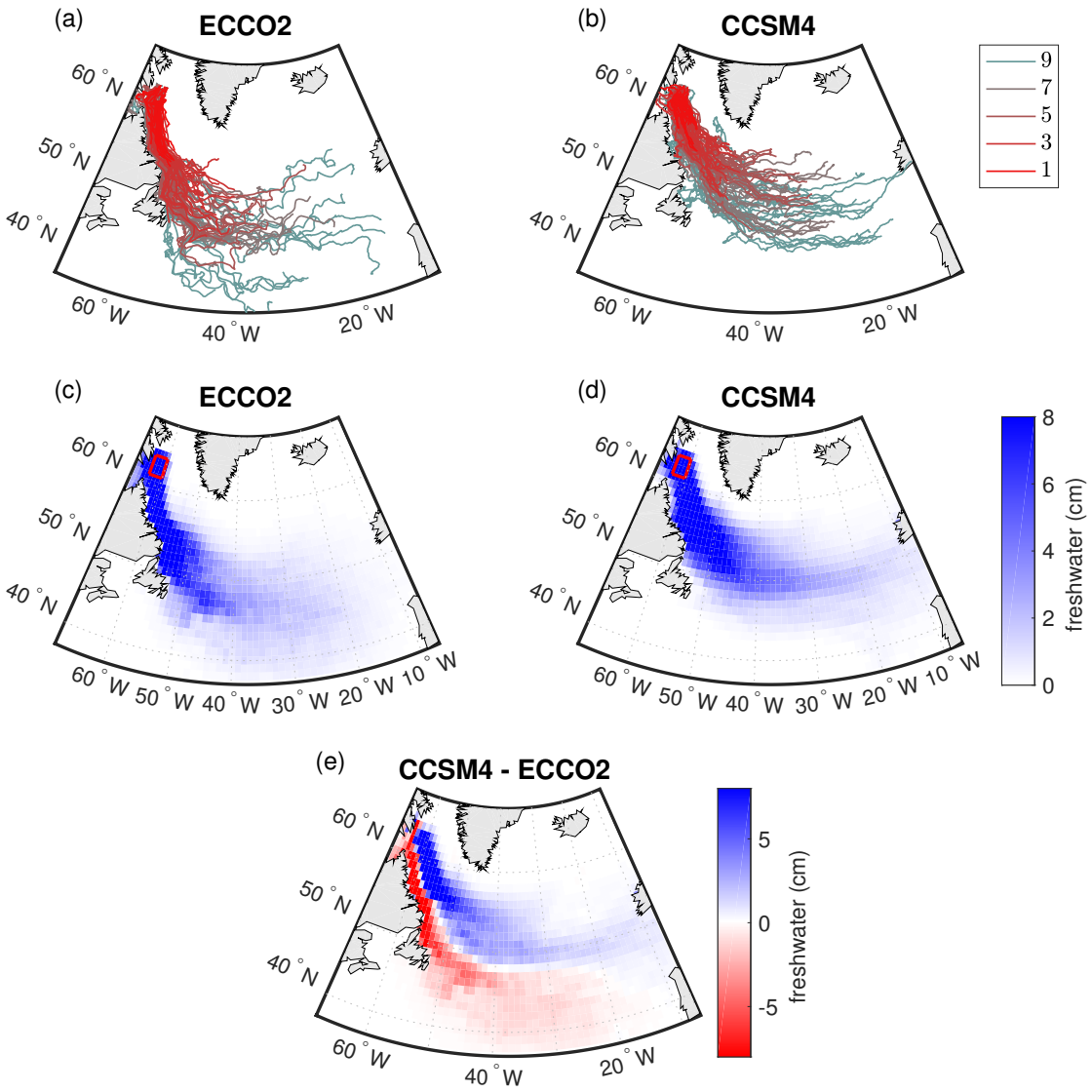

Figure S4. As Fig. 1 in the main text, but using the representation of M_e from J09. Following Bigg et al. (1997), J09 also take $M_e = S_s/2$ with M_e in m/d. However, they specify a different dependence of S_s on wind speed: $S_s = -5 + (32 + 2|\vec{V}_a|)^{1/2}$, where $|\vec{V}_a|$ is given in km/h. We rewrite this using dimensional parameters in the main text.

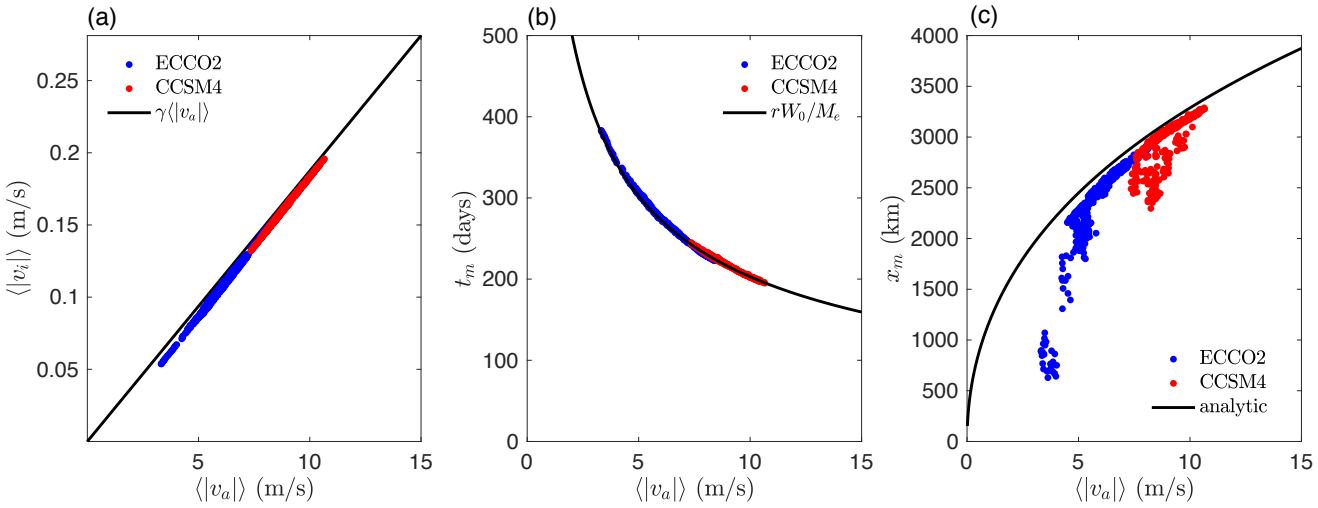

Figure S5. As Fig. 4 in the main text, but for size class 5.

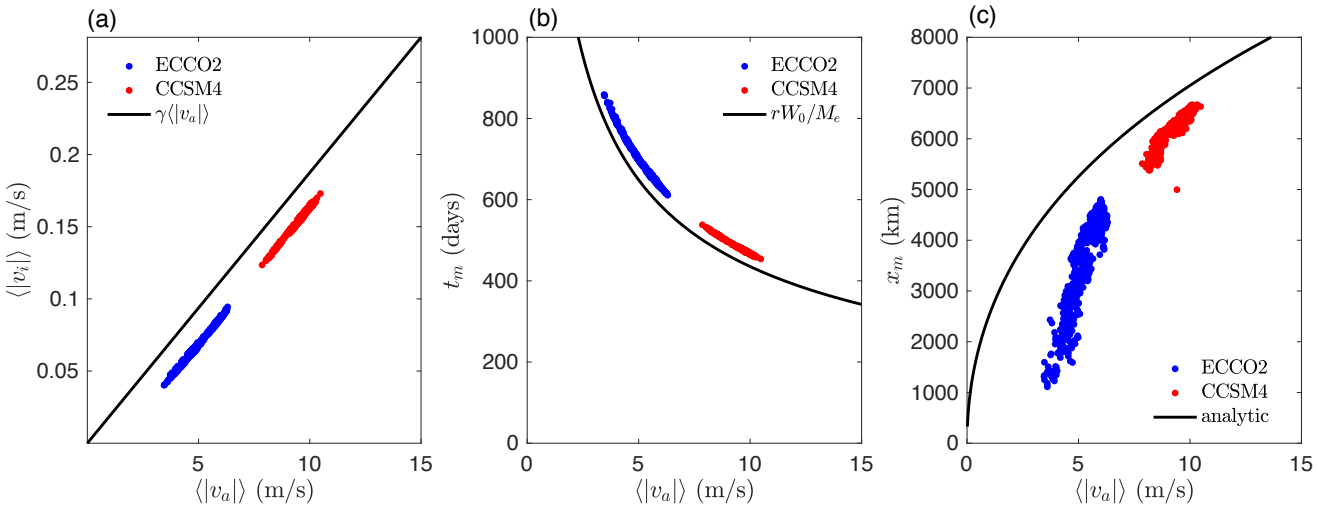

Figure S6. As Fig. 4 in the main text, but for size class 10. Note that here $r = 1.25$, since $r = 5/4 + H_0/2W_0$, and $H_0/W_0 = 0.33$ for size class 10.